Revista Brasileira de Física, Vol. 17, n? *3,* 1987

Metastable Cadmium (5^3P_1) Production in the Cd+ – Na Charge-Exchange Collision

L.F.S. COELHO
Departamento de Fikica, Universi&& Federal do Rio de Janeiro, Caixa Posral68528, Rio de Janeiro, 21944, RJ, Brasil

Recebido em 25 *de novembro de* 1985. *Versão revista em* 27 *de março de* 1987

Abstract The 326.1 nm emission cross section for the c011ision process Cd+ +Na + ~ d (5 +~ ~~a +w)as measured in the energy range 1.5-4.9 keV. It decreases monotonically from 5 to 2xlO-l~cm2. Due to a near degeneracy in energy, this channel presents a much larger cross section than a11 others (except 5 3 and 5-3 ~ 2which are highly metastable). This justifies the neglect of the cascade mechanism for populating the 5 3 ~ state and, consequently, allows the identification of the 326.1 nm emission cross section with the s3P1 charge-exchange excitation cross section. The measured values agree well with theoretical estimates obtained with Olson's *model* for near-resonant charge exchange.

1. INTRODUCTION

The collision process studied here is

$$Cd^+(5^2S_{1/2}) + Na(3^2S_{1/2}) \rightarrow Cd(5^3P_1) + Na^+(2^1S_0) \qquad (1)$$

where all particles, except the cadmium atom, are in their ground states. The *projectile* (the cadmium ion) has laboratory energy in the range 1.5 - 4.9 keV, well inside the low energy region ($v \ll \alpha c$). This is a near-resonant charge-exchange collision.

This work is divided into four sections: theory, experimental arrangement, results and conclusions. In the first section we discuss the particular features of the Cd^+-Na case, with theoretical estimates of the cross section of interest (for a recent review of low energy atomic collisions see Delos[1]. Next, we describe the apparatus and the several calibration procedures. Finally we present the results, the conclusions and an appendix with the cross section formulae.

2. CROSS SECTION CALCULATIONS

Low energy collisions $A+B \rightarrow C+D$ are usually classified by their

energy defect ΔE_∞. This parameter is the limit, at large inter-nuclear separations R, of the difference $\Delta E(R)$ between potential energies of the incoming -AB- and outgoing -CD- quasimlecules:

$$\Delta E_\infty = \lim_{R\to\infty} \Delta E(R) \tag{2a}$$

where

$$\Delta E(R) = E_P(A+B) - E_P(C+D) \tag{2b}$$

As the interatomic potentials vanish at large R values, one obtains

$$\Delta E_\infty = E_P(A) + E_P(B) - E_P(C) - E_P(D) \tag{2c}$$

A collision is near-resonant[2-13] when ΔE_∞ is small. Demkov has shown that, in this case, a transition happens when R lies in a narrow region around a critical internuclear distance R_c, such that the coupling matrix element $H_{12}(R)$ satisfies

$$H_{12}(R_c) = \frac{1}{2}\,\Delta E(R_c) \tag{2d}$$

A good approximation for $\Delta E(R)$ is

$$\Delta E(R) = \Delta E_\infty + \frac{\Delta\alpha}{R} \tag{2e}$$

$\Delta\alpha$ being the difference between the polarizabilities of the neutral atoms. If ΔE_∞ is smaller than 0.5 eV, R_C is so large that the second term in the RHS of (2e) may be neglected[3], as it amunts to a correction of less than 10%.

Olson *et al*[4] showed that $H_{12}(R)$ could be fitted by a semi-empirical function which reproduced 83% of the data within a factor of 3. This allows one to solve equation (2d) obtainning R_c, and also to obtain its lower and upper bounds, respectively R_c'' and R_c':

$$H_{12}(R_c) = \frac{1}{2}\,\Delta E_\infty \tag{3a}$$

$$3H_{12}(R_c') = \frac{1}{2}\,\Delta E_\infty \tag{3b}$$

$$\frac{1}{3}\,H_{12}(R_c'') = \frac{1}{2}\,\Delta E_\infty$$

In a subsequent paper Olson[4] calculated a universal charge exchange cross section (see appendix):

$$\sigma(v) = (\pi R_c^2/2) f(kv) \quad , \tag{4a}$$

where f was a tabulated function and k a parameter with a given analytical dependence on ΔE_∞. The function f presented a maximum value of 1.08 at

$$v_{max}(\mathrm{cm/s}) = 1.45 \times 10^8 \ (\Delta E_\infty / I^{1/2}) \tag{4b}$$

where ΔE_∞ and I, the ionization potential of the incoming atom, are given in eV.

For the collision described by eq.(1), four quasirnolecular levels are very close to each other, favouring charge exchange into the 5^3P levels, (see fig.1). The energy defects for leaving the cadmiumatom in the 5^3P_0, 5^3P_1 or 5^3P_2 states are, respectively, 0.120, 0.053 and -0.067 eV, while the defect is 3.854 eV for the ground state and larger than 1.5 eV for any other excited state. Transitions at R=0 cannot be ruled out but they populate rnainly the ground state (thereby not producing cascades). In any case, these processes have small cross sections associated with them. Another possibility is that of a crossing at a finite R between the elastic and the 5^1P_1 charge exchange channels, but the decay of 5^1P_1 does not populate the 5^3P levels and again there is no cascade contribution. As the croçs sections for slow collision without level crossing are much smaller than otherwise, we may neglect the cascade population of the 5^3P states and consider the cross sections for the 326.1 nm emission and for $Cd(5^3P_1)$ production through charge exchange as identical to each other.

One needs to be sure that eq.(1) describes well the *collision*; thus, each of its terms deserves some comments, as follows. I) $Cd^+(^2S_{1/2})$: the Cd^+ ions are in the ground state (the longest lived metastable state, $Cd^+(^2D_{5/2})$, larting for 0.79µs, will decay before reaching the collision cell). II) $Na(3^2S_{1/2})$: these atoms are in the ground state because the cell temperature is less than 600°K (average kinetic energy of 0.07 eV), while the first excited level has an energy of 2 eV. III) $Cd(5^3P_1)$:

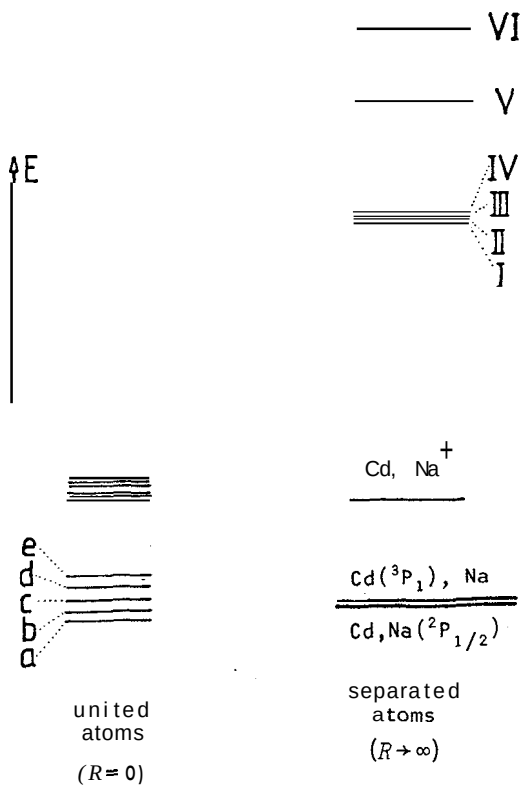

Fig.1 - Quasi-molecular energy levels of the $CdNa^+$ system I) $Cd(5^3P_0)$, Na^+_g (g denotes ground state); II) $Cd(5^3P_1)$, Na^+_g; III) Cd^+_g, Na_g; IV) $Cd(5^3P_2)$, Na^+_g; V) $Cd(5^1P_1)$, Na^+_g; VI) $Cd(6^3S_1)$, Na^+_g. a) $Pr^+(^5I_4)$; b) $Pr^+(^5I_5)$; c) $Pr^+(^5I_6)$; d) $Pr^+(^5I_7)$; e) $Pr^+(^5I_8)$.

these atoms are detected through the emission of light during their decay to the ground state. IV) $Na^+(2^1S_0)$: any possibility other than the ground state for this ion will result in energy defects 10^3 times larger (the energy of the Na^+ first excited state is 32 eV, compared with an energy defect of 53 MeV for the process (1)).

All 5^3P states of Cd are metastable, not being allowed to decay into the ground state 5^1S_0 because ΔS is nonzero. The partial breakdown of the LS coupling for heavy atoms mixes the 5^1P_1 and 5^3P_1 states, the latter decaying with a large but finite lifetime[14] (2.39μs). The 5^3P_0 and 5^3P_2 states decay much more slowly[15] (90 and 140μs, respectively) because their mixing with 5^1P_1 and 5^3P_1 is very small (nonzero ΔJ). The slowest cadmium ions have 1.5 keV kinetic energy, resulting in a decay length larger than 10 m and in a decay probability for 5^3P_0 and

5^3P_2 smaller than 0.2×10^{-6} inside the accelerator, whose length is of the order of 2m. These large lifetimes make it possible to neglect the decay of $5^3P_{0,2}$.

Solving computationally eq. (3a) for $Cd(5^3P_J)$ we obtain R_c equal to 8.638. 7.528 and 8.38, respectively for J=1,0 and 2, leading to

$$\sigma_{max} = \begin{cases} (5^3P_1) = 4.7 \times 10^{-15}\ cm^2 \\ (5^3P_0) = 3.6 \times 10^{-15}\ cm^2 \\ (5^3P_2) = 4.3 \times 10^{-15}\ cm^2 \end{cases} \qquad (6)$$

Taking into account the uncertainty in $H_{12}(R)$, eqs. (3b) and (3c) give a lower bound $R_c'' = 6.898$ and an upper bound $R_c' = 10.07\text{Å}$ and 5^3P_1. Within 83% probability, these values lead to the 5^3P_1 cross section maximum lying between 3.0 and 6.4×10^{-15} cm^2. Inserting the most probable R_c value for each 5^3P_J state into eq. (4a) we obtain the respective cross (see figure 5).

Near-resonant charge-exchange collisions are easier to describe for the *quasi one electron* systems, presenting one valence electron and two closed cores, the typical example being an alkali ion-alkali atom collision. As the initial configurations, the Cd^+ ion and the Na atom, are $(5s)^1$ and $(3s)^1$ respectively, our system is a *quasi two-electron* one. Almost all the theoretical and experimental effort[2-13] has been placed on the simpler *quasi one-electron* systems, particularly on the alkali dimers. Using simple analytical expressions for the coupling matrix element H_{12}, base on hydrogenic wave functions, one is able to obtain relatively simple formulae for the cross section[2-4,8-13]. Specific cases[11,13] may be more accurately calculated write LCAO molecular wave functions in order to obtain the many interacting hamiltonian matrix elements (in some cases using multi-state approximations but with no great improvement over 2- on 3-state LCAO calculations[13]).

An important parameter v_{max}. For $v>v_{max}$ the cross section is expected to decline slowly, being nearly equal to the exactly resonant cross section (except for a statistical factor), and declining sharply

for velocities below v_{max}. Based on the adiabatic rule proposed by Massey[5]

$$v_{max} = \alpha |\Delta E_{\infty}| / h \qquad (7)$$

Hasted[6] obtained the best fit of eq. (7) to the experimental data for $\alpha = 7\text{Å}$. In our case this gives $E_{max} = 47$ eV.

Hasted also noticed the inadequacy of eq. (7) to describe experiments with heavy ion projectiles the obtained an empirical expression for v_{max} which gives in the present case $E_{max} = 280$ eV. Olson[4] obtained a good fit for v_{max} by parametrizing it against $\Delta E_{\infty}/(I)^{1/2}$, similarly to a two-regime fit made by Perel and Daley[7]; their results are respectively E_{max} 669 and 1540 eV. Rapp and Francis[8] follows the Massey-Hasted adiabatic criterion as well as Demkov[2] who nevertheless suggests a equal to the radius of the outer electron state. Demkov[2] and Rapp and Francis[8], due to the numerical complexity, stated thecriterion without actually comparing its prediction with their cross section calculations. Lee and Hasted[9], after simplifying Rapp and Francis[8] equations, obtained an analytical expression for v_{max} giving, in our case, $E_{max} = 840$ eV.

It is not possible in the present experiment to test the above values for E_{max} as the beam optics does not allow for beam energies below 1500 eV. This procedure would be more decisive than the measurement of σ for $v > v_{max}$ where the predictions of the different models present a much smaller disagreement among themselves. Nevertheless, it is possible to estimate the cross section using, besides Olson's already mentioned calculations[4], more refined ones by Bottcher[3] and Dinterman and Delos[10].

Bottcher[3] proposed an expression for $H_{12}(r)$ which, when inserted into eq. (3a), results in a cross section maximum equal to 1.6×10^{-15} cm^2. This valuemay be compared with Olson's value of 4.7×10^{-15} cm^2, given by eq. (6); it is important to notice the greater reliability of the latter, due to the presence of two empirically adjusted parameters ion the expression for $H_{12}(r)$. Dinterman and Delos[10] propose

$$H_{12}(r) = A\, e^{-\lambda r} ,$$

A and A being obtained from exact potential energy curves[3,...]. Their results agree well with the observed the Li^+-Na, charge exchange cross section. Olson's result underestimates this cross section by nearly 20% because of the use of a universal $H_{12}(r)$ expression. As the potential energy curves for the $(Cd\text{-}Na)^+$ molecule have not, as farasthe author is aware, been calculated, Dinterrnan and Delos' method cannotbe applied here.

Another purpose of this work was to look for periodic oscillations in the total cross section. The sirnple two-state case does not allow such oscillations, giving instead a broad and smooth cross section curve. The first experimental evidence of this phenomenon was obtained[16] in 1967, followed by qualitative[17] and quantitative[18] models. These oscillations are produced by interference between three potential energy curves during the collision.

In 1972 Shpenik and co-workers[19] measured relative cross section values, in the 0-1 keV range, for direct excitation of $Cd(5^3P_1)$

$$Na^+ + Cd \rightarrow Na^+ + Cd(5^3P_1) \qquad (8)$$

This is a non-resonant process and a smooth energy dependence was obtained. It was measured in absolute values by Aquilanti and co-workers[20] in 1981, confirrning the lack of structure and the absenceof polarization. These results were interpreted as due to a weak spin-orbit coupling in the cadmium atom, leading to Ω (J projection on the interatomic axis) not being a good quantum number. This may explain the absence of polarization (a statistical population for the sublevels with $m_J = 0, \pm 1$) but not the discrepancies with their own results[21] for direct excitation of $Hg(6^3P_1)$. In this metastable state of rnercury there were strong cross section oscillations, attributed to interference with nearby channels (probably leading to $6^3P_{0,2}$). The cadmium and mercury atomic structures are very similar and it is hard to understand the existence of oscillations only in one case. The non-existence of structure in the $Cd(5^3P_1)$ direct excitation cross section, as verified by Shpenik and Aquilanti, aroused interest in the charge exchange channel.

3. APPARATUS DESCRIPTION AND EXPERIMENTAL PROCEDURES

3.1 - General description of the apparatus

The experimental arrangements is shown in figure 2, being fully described elsewhere[22]. Cadmium ions are produced in the RF ion source. They are extracted, accelerated and focused by fhree cylindrical electrodes. The target cell consists of a collision region 1.78 cm long and an oven, where atomic sodium is generated. The excited cadmium atoms in the 5^3P_1 state decay, with decay lengths going from 12.1 to 21.9 cm (for beam energies ranging from 1.5 to 4.9 keV). The 326.1 nm radiation is detected by two photomultipliers (EMI9689QB) with broad band filters in front of each of them. To obtain the cadmium beam, pellets are placed inside the RF ion source.

Impurities in the cadmium plasma are detected by the spectral analysis of the visible light emitted. In a first stage there is an, auxiliary helium discharge and it is possible to have HeI and II atomic lines mixed with molecular spectra continua from residual gases. The helium lines disappear a few seconds after turning off the helium supply (the partial pressure also falls to zero). Data are taken when there are only CdI lines,

The target cell is formed by a heater, a collision region, an oven and a cylindrical support (see figure 3). A horizontal cylindrical hole of 1.27 cm diameter is bored through it, being ended by two caps (1 mm collimation diameter) and defining a collision region 1.78 cm long. The oven is made in molybdenum, with a copper disc around it. A thermocouple fitted to the disc (copper-constantan) permits the determination of the vapour pressure and the target density. The thermal EMF measurement has a 2μV uncertainty (less than 0.1°C error).

The target element is obtained by the thermal decornposition of sodium azide (NaN_3), which happens at 275°C. This method makes easy the loading (there is no oxidation) and allows the baking of the cell at a temperature below decomposition, increasing the vacuum quality during operation. After decomposition the sodium azide, the cell is allowed to cool. The calculated vapour pressure was checked in three preliminary runs by the following experiment: a surface ionization detector was

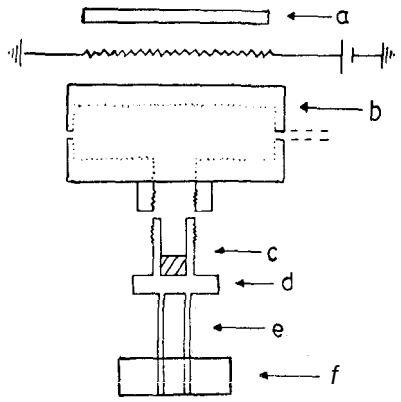

Fig.3 - Scheme of the collision cell. a) top plate (stainless steel); b) collision region (stainless steel); c) molybdenum oven; d) copper disc; e) hollow cilinder (stainless steel); f) cooper block cooled to 12°C.

placed in front of one of the cell openings, measuring the sodium flow in relative units. The ration of this flow (proportional to the target density) to the calculated vapour pressure is constant within ±5% for densities varying by a factor of 1000, showing a very good agreement between calculatèd and measured target densities.

3.2 - Detection and calibration procedures

The 326.1 nm photons are detected by two photornultipliers placed opposite to each other and orthogonal to the beam. The anode current is fed into an operational amplifier with a feedback resistor of 1 MR, resulting in a current/voltage transducing ratio of 1.00 V/μA.

The number of photons arriving at the photomultiplier window is given by

$$I_T = \int_z \int_S \frac{dN}{dz}\, dz\, \frac{d\Omega}{4\pi} \qquad (9)$$

where z is the beam axis, S the exposed area of the window, N the flow of atoms in the 5^3P_1 state and R the solid angle defined by a point of the beam axis and the area S. An analytical expression was obtained[23] for I_T, namely,

$$I_T = 10^{-3}\, N_0\, \exp(-L/z_0)\{3.18 + 3.96\, z_0^{-2}\} z_0^{-1} \qquad (10)$$

where z_0 (in cm) is the decay length of the 5^3P_1 rnetastables, N_0 their

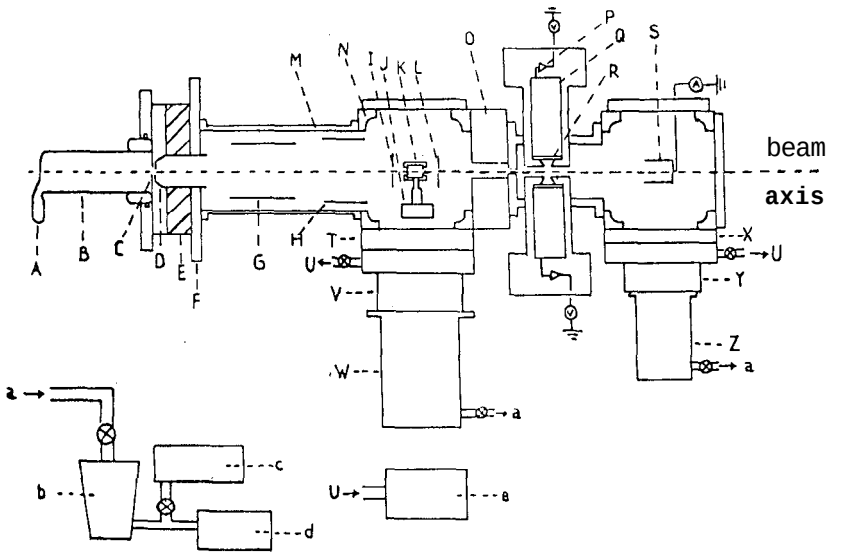

Fig.2 - Experimental arrangement. A - Cadmium reservoir; B - Ion source (RF driven); C - Plasma potential electrode; D - Extraction electrode; E - Magnet (windings inside the hatched region); F - Heat dissipator for the magnetic; G - Focusing electrode; H - Grounded electrode; I - Collimator (0.79 mm diameter, water cooled); J - Copper block (also, water cooled); K - Target cell; L - Collimator (3.05 mm diameter, watercooled); M - Brass pipe (10 cm inner diameter); N - Aluminum alloy cube (Dural) (15 cm, with three 10 cm I.D. holes bored through); O - Slit system (optional collimator); P - Operational Amplifier (transduces the anode current to voltage); Q - Photomultiplier tube (EMI 9689QB); R - Broad band filter, with a 3.05 mm collimator; S - Faraday cup; T - Butterfly valve; U - Output to the roughing rotary pump; V - Liquid N_2 trap; W - E06 diffusion pump; X - Butterfly valve; Y - Water cooled baffle; Z - 403 diffusion pump; a - Outlet of both diffusion pumps; b - Booster pump; c - Backing rotary pump (optional.); d - Backing rotary pump; e - Roughing rotary pump. (The holder of the target assembly was omitted for reasons of clarity).

flow through the cell exit, and L the distance from this exit to the centre of the detection region (16.9 cm). For low target densities, N_0 is given by

$$N_0 = \frac{I}{e} n \sigma L_C \qquad (11)$$

where I is the Cd^+ current, e the electron charge, a the cross section, n the average target density in the beam path inside the cell and L_c the cell effective length, defined as the density integrated along all the beam path and divided by n (L_c is nearly equal to the sum of the geometric length of the cell and the entrance and the exit diameters).

A broad band filter is used in order to select a bandwidth centered at 3250Å (model UG-11, Oriel), cutting off completely light outside the 2600-3900Å range.

The radiation reaches the photocathode at angles smaller than 30^o. Below this angle, the reflection losses are small and fairly constant (reflectivity at 30^o is 4% larger than at normal incidence). To achieve this angle limitation a 3.2 mm collimator was glued to the filter and another placed farther apart. This 3.2 mm collimator defines the exposed area.

The overall efficiency of detection E for the system formed by photomultiplier, filter and the 3.2 mm collimator is obtained using a calibrated D_2 lamp (obtained from NPL, Teddington, UK). Its value is $(3.00 \pm 0.03) \times 10^6$ for the operation photomultiplier bias (1.15 kV) and it is defined as the number of electrons leaving the photomultiplier anode per incoming photon, being then the product of the window and the filter transmissivities, the cathode quantum efficiency and the photomultiplier gain.

The measured signal is given by the product $I_T \varepsilon$; using eqs. (10) and (11) the charge exchange cross section is

$$\sigma = \frac{(S/I)}{nF} \qquad (12)$$

where S is the transducer output, I is the beam current and F the product of the remaining constants.

3.3 - Measurements procedures

For a given target density the beam energy is lowered from 4.9 to 1.5 keV by steps of 0.1 keV. The signal intensity for each energy value (photomultiplier output) is divided by the beam current and this normalized signal plotted versus the target density (a typical graph is shown in figure 4). From the low density limit of the derivative we obtain the cross section for process (1). The linearity at low target densities justifies the neglect of cascading, as cascades would cause a parabolic dependence.

In order to obtain a meaningful total cross section measurement one needs the detection of the incident Cd^+ beam and the scattered $Cd(5^3P_1)$ beam. The incident beam is collimated before reaching the cell by a 0.79 mm collimator and the entrance and exit of the cell have 1.00 mm diameter. The alignment of collimator, cell and ion source extraction is done with a He-Ne laser. After leaving the target the beam crosses one collimator (6.35 mm) and the photomultiplier detection region (12.70 mm wide) before reaching the Faraday cup. This is enough to accommodate space-charge effects (even in the lowest energy - 1.5 keV - and without neutralization by electron trapping). The angular spread of the $Cd(5^3P_1)$ beam is negligible as the beam is focused at the target (see figure 2), in order to maximize the current at the Faraday cup, resulting in a cylindrical beam envelope which suffers the collimation before the target. The angular spread of the $Cd(5^3P_1)$ beam is due to the collision process and any finite cell exit diameter will cause losses. The centre of the target and the cell exit define a 3.2^o angle. As the charge exchange cross section presents a maximum for large impact pararneters (where the pseudo-crossing occurs), the angular spread of the scattered projectile is small (of order 1^o). For instance, one such process is the near-resonant charge exchange Li^+-Na (ΔE_{cm} = 0.253 eV). Los[23] measured its differential cross section at 0.5 keV obtaining non-zero values onlyfor angles smaller than 0.3^o. To estimate the importance of the $Cd(5^3P_1)$ losses the cell and collirnator system were rotated, allowing an angle (up to 1.2^o) between the incident ions and the scattered metastables. Within ±10% there is no variation of the normal ized signal, showing that most of the atoms are scattered by less than 1^o. Thus the contribution

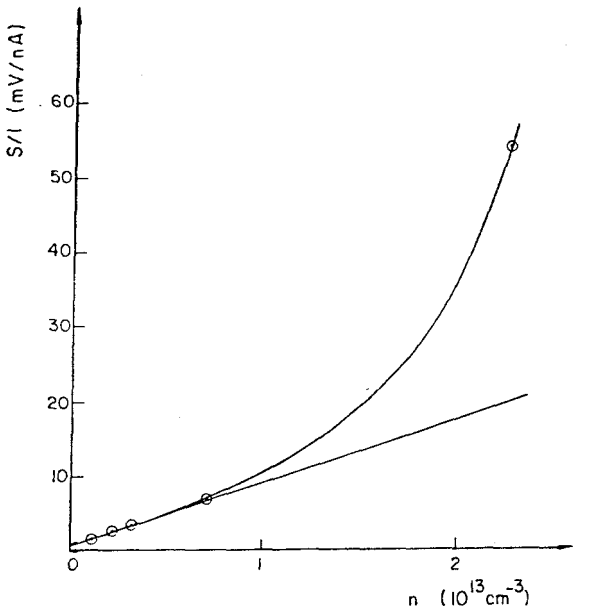

Fig.4 - Typical curve of normalized signal (mV/nA) versus target density (10^{13} cm^{-3}) (E = 3.5 keV).

of the angular spread to the error in the cross section rneasurement is estirnated as 10%.

3.4 - Error analysis

Equation (12) must be corrected for several effects which, besides changing its measured value, will increase its standard deviation.

Each point in the normalized signal (S/I) versus target density (n) graph is an average over several values of S/I for given target density and beam energy. Points scattered more than 5% from this average were not considered (they appeared when the ion beam current was either too srnall or, due to ion source condensation, too unstable).

As runs for different target densities were performed at different dates, there are different plasma boundary conditions in the ion source. This may cause a maximum beam displacement of ±0.4 mm in front of the photornultiplier, introducing a 3.5% contribution to the standard

deviation.

The target pressure is obtained from the thermocouple EMF using semi-empirical vapour pressure curves[24]. These curves agree with other curves[25] within $\pm 1.5^{o}K$. At $500^{o}K$, this discrepancy would cause a 7.5% error in the density. A quantitative estimate of this errorwasobtained with an auxiliary experiment, as already described in 3.1, yielding a value of 5%.

Other less important effects are: the collision region iswarmer than the oven, as it is closer to the heater; the interna1 gas conductances of the cell being non-infinite, there is a decrease in the gas density as it flows from the oven on the cell opening. The temperature gradient was measured and, for the temperature range used, results in the actual density being larger than that in the oven by amounts from 1 to 3%. The gas conductance effect is smaller, causing the average density of the collision region to be 0.5% lower than calculated. These two secondary effects were accounted for when calculating the sodium density in the collision region.

The overall standard deviation of each individual point of the graph is 6.5%, but the two main effects - beam displacement and oven temperatura - are partially compensated when the slope is the low density region is obtained. The worst estimate for the standard deviation of the line slope is then equal to 6.5%.

The length L_c in expression (11) must take into account the beaming of the outgoing sodium vapour flow. The pressure does not fall to zero immediately after leaving the cell and the effective L_c is the geometric value (17.8 mm) added to the sum of the cell openingdiameters (2.0 mm). This increases the cell length by 11%± 1%, introducing a 1% error.

Besides these sources of error resulting in a standard deviation of 4.7%, there are two others: the anisotropy of emission (non-zero polarization) and the angular scattering of metastables.

The detection system accepts light emitted at angles (with the beam direction) ranging from 60^{o} to 120^{o}. The angular anisotropy introduced by an eventual polarization P of the $5^{3}P_{1}$ state would result in a difference between the measured signal and the isotropic one

$$\frac{\langle S(\theta)\rangle}{(S/4\pi)} = \left[\frac{1-0.09P}{1P}\right] \qquad (13)$$

where S is the signal integrated over all directions. If P is -1 or +1 the correction factor on the RHS of eq. (13) will be, respectively, 0.82 and 1.36. As this anisotropy was not included in the solid angle calculation, the measured cross section should be divided by a number lying between 0.82 and 1.36. A semi-classical argument points to P equal to-1: charge exchange collisions normally happen at large impact parameters, where the two quasi-molecule energy potential curves have a pseudo-crossing at R_c. As R_C is large the electrons will come from the target to the projectile mostly at a right angle to the beam, populating preferentially the two $^3P_1$ orbitals perpendicular to the beam and resulting in P=-1. Nevertheless, a very similar collision process[21] pointed to the absence of polarization of the 326.1 nm light. As the P value lies between 0 and -1 (probably closer to zero) the values calculated assuming isotropy, may at worst case be divided by 0.82 (a 22% increase) and at best remain unchanged, then introducing an uncertainty of 11% and an increase of 11% in the absolute values of the cross sections.

A last error source, already mentioned in 3.3, is the angular scattering of the metastables and contributes with ±10%.

Tha accumulated error (an overestimate of the standard deviation) is due to the angular scattering losses, the polarization anisotropy, the vapour pressure curves, the statistics of measurement andthe beam displacement effect. As these effects are independent, and assuming gaussian distributions, the overestimated total standard deviation is 15%.

4. RESULTS AND CONCLUSIONS

The experimental cross sections are displayed in figure 5, together with our theoretical calculations based on the model presented by Olson[3], showing a very good agreement.

A more accurate calculation of a would take into account the of four nearby quasi-molecular levels (see figure 1) and not only pairs

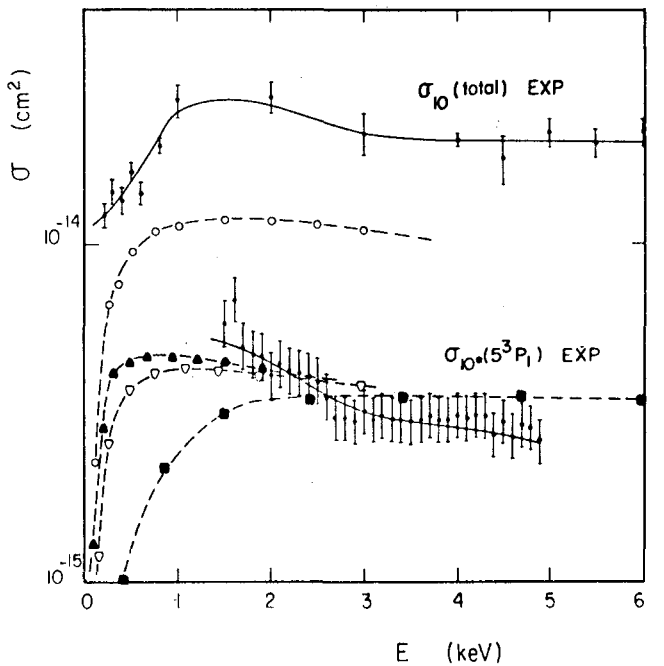

Fig.5 - Cross section σ_{10*} for $Cd(5^3P_1)$ production (25%) (this paper, o—o); cross section σ_{10} for total charge exchange (Martin *et al*[31] o—o); theoretical estimates for 5^3P_0, 5^3P_1 and 5^3P_2 production cross sections respectively indicated by V--V, A--A and -- (this paper) and their sum indicated by o--o. The continuous lines passed through the points are to give a visual help.

of levels (initially Cd^+ and Na in their ground states and finally $Cd(5^3P_J)$ and Na^+ ($^1S_0$). This may change the theoretical values given by eq. (6) and figure 5 but not their order of magnitude.

In the section 2 we mentioned the possibility of periodic structures of the cross section[16], explained by the three state model[17,18]. Here we will briefly discuss this model in order to understand our case, with four nearby competing channels. In a collision with three channels (two inelastic and one elastic), the two inelastic potential energy curves being very near each other, there are transitions at the crossing R'_c between the elastic and any of inelastic states, and at the crossing R''_c

between the inelastic states. As the colliding particles approach and depart, they may cross R'_C and R''_C twice, and one has several ways to go from the elastic, for example, to the first inelastic, with interference between them. The main parameter is the quotient of the energy defect and the velocity, and the cross section has oscillatory terms with argument roughly proportional to this parameter. If the energy defect is small, the oscillations in $\sigma(E)$ are broader and more intense, being easier to detect.

The existence of four nearby competing channels produces an interference pattern more complex than that of the three state model[18]. This may be the reason for Shpenik and Aquilanti not observing clear oscillations in the direct excitation of $Cd(5^3P_1)$ (non-resonant process, with three nearby channels), while Aquilanti measured strong oscillations for the direct excitation of the metastable $Hg(6^3P_1)$. In mercury the gaps 6^3P_1-6^3P_0 and 6^3P_1-6^3P_2 are respectively 3.3 and 4.8 times larger than the corresponding gaps in cadmium, producing in this latter case an interference pattern much weaker than in the former.

The presence of several channels destroys the coherence of the 5^3P_1 light (as verified by Aquilanti in the direct excitation of Cd) and the interference pattern (also verifies by Aquilanti and Shpenik). This is even more evident for the charge-exchange excitation of $Cd(5^3P_1)$ instead of three there are four nearby channels); oscillations in the total cross section were not experimentally observed here.

As far as we are aware, there are no measurements of low energy charge-exchange collisions where the collision system is a quasi-two-electron one and the projectile is left in an excited state. There are two sorts of similar experiments however: low energy direct excitation collisions with the collision system being either quasi-one-electron[26] or quasi-two-electron[27-29]; and low energy charge-exchange collisions with a quasi-one electron collision system and the projectile in an excited final state.

Direct excitation in quasi-one-electrom system was thoroughly studied by the Copenhagen group and they present a recent review[26]. Afterwards they presented experimental results for direct excitation in the

quasi-two-electron system $(LiNa)^{27}$. Their own theoretical description[28] and the one proposed by Kimura and Olson[29], while accounting for the presence of two cross section maxima (also present in quasi-one- electron collision systems), fail to describe their position and intensity. The higher energy maximum may be roughly described by the Massey adiabatic criterion, which involves the valence electrons. The other maximum is associated with small impact parameters and corresponds to the interpenetration of the atomic cores promoting one inner electron of one atom to a valence position in the other. As Andersen[26] points out, this second mechanism is more dependent on the specific collision system, as it cannot be explained with hydrogenic models, and obviously it is harder to calculate. The already mentioned measurements of the direct excitation of Cd by Na^+ projectiles related to the quasi-two-electron system $(CdNa)^+$ (in our case the energy range for charge exchange excitation of Cd^+ lay above the Massey maximum and we did not expect to see this structure).

In order to understand low energy charge-exchange collisions, leading to the excitation of the projectile, a system well studied recently[30] is:

$$H^+ + Na \rightarrow H(n=2) + Na^+ .$$

Atomic and molecular orbitals were used. We observe disagreements between the experiments, and between experiments and theory. This process, similarly to the direct excitation ones related above, is non-resonant but presents an energy defect close to 1 eV. The energy defects larger than in our case lead to the *Demkov crossings* occuring at small R values, and hence the hydrogenic atomic orbitals give a worse description of the valence electrons (in our case, for instance, the Olson formula for $H_{12}(R)$ is based on hydrogenic systems). Besides this extra difficulty, which leads to the use of molecular orbitals, the cross section for non-resonant processes is smaller, which may account for discrepancies between the experimental data.

Figure 5 shows our experimental results for charge exchange into the 5^3P_1 state, experimental results obtained by Martin, McCullough and Gilbody[31] for charge exchange into all states and our

theoretical estimates for $\sigma(^3P_1)$ and $\sigma(5^3P_{0,1,2})$. As faras the author is concerned these unpublished results are, besides ours, the only ones involving charge exchange in the $(CdNa)^+$ system.

Our experimental points agree reasonably well withtheestimates of 5^3P_1 charge-exchange cross section, presenting however a sharper increase towards low energies. On the other hand, considering the semi-empirical nature of the coupling matrix element $H_{12}(R)$, which as pointed out in the second part of this paper introduces an error of nearly 30% in the theoretical estimates the agreement is very satisfactory. The total charge-exchange values of Martin *et al*[26] are compared with the sum of the charge-exchange cross sections for $5^3P_{0,1,2}$, as calculated using Olson's model, being found to be nearly twice these theoretical values. This suggests a breakdown of the already mentioned assumption of the Demkov model (transition between two nearby quasi-molecular states), a rough approximation when there are, besides the elastic, three near--resonant inelastic channels.

The author wishes to thank Dr. J.M. Pendlebury for suggesting this subject as part of a DPhil Thesis at Sussex University and for helpful comments at severa1 stages of this work; Prof. H.B. Gilbody for sending unpublished results[31] for the charge exchange of Cd^+ into all states of the cadmium atom; Dr. V. Aquilanti for sending a complete collection of papers published by his group in Cd, Hgandalkali collisions. He also acknowledges one year of financial assistance by the Pontifícia Universidade Católica do Rio de Janeiro (PUC-RJ) and 14 rnonth assistance from the Conselho Nacional de Pesquisas (CNPq).

APPENDIX

Olson[4] calculated a universal expression for the near - resonant charge-exchange cross section

$$Q(v) = 4\pi R_c^2 \int_1^\infty \frac{dx\ e^{-\delta x}}{x^3(1 + e^{-\delta x})^2} \qquad (14a)$$

or

$$Q(v) = \frac{1}{2}\pi R_c^2\, Q^*(\delta^{-1}) , \qquad (14b)$$

Q^* and δ^{-1} being, respectively, the reduced cross section and the reduced velocity.

As already mentioned the crossing point R_c is obtained by solving

$$2H_{12}(R_c) = \Delta E(R_c) \simeq \Delta E_\infty \tag{15a}$$

A semiempirical expression[4] for $H_{12}(R)$ gives

$$H_{12}(R) = (I_1 I_2)^{1/2} R^* e^{-0.86R^*} \tag{15b}$$

where

$$R^* = \frac{1}{2}\left[(2I_1)^{1/2} + (2I_2)^{1/2}\right] R = \lambda R/0.86 \tag{15c}$$

I_1 and I_2 are the effective ionization potentials of the initial and final atoms and all quantities are given in atomic unities. To obtain the reduced velocity one uses

$$\delta^{-1} = \frac{2\hbar\lambda}{\pi \Delta E(R_c)}\, v \tag{16}$$

where v is the projectile velocity.

The resulting $Q^*(\delta^{-1})$ values[4] are shown in table 1.

Table I - Calculated reduced cross section Q^* versus reduced velocity δ^{-1} (ref. 4).

δ^{-1}	Q^*
0.5	0.03
1.0	0.30
1.5	0.66
2.0	0.95
2.5	1.05
3.0	1.08
3.5	1.07
4.0	1.05
4.5	1.02
5.0	0.99

REFERENCES

1. J.B. Delos, Rev. Mod. Phys. 53, 287 (1981).
2. Yu. N. Demkov, Sov. Phys. JETP *18*, 138 (1964).
3. C. Bottcher and M. Oppenheirner, J. Phys. B*5*, 492 (1972); C.Bottcher, J. Phys. B*11*, 507 (1978).
4. R.E. Olson, F.T. Smith and E. Bauer, Appl. Optics 10, 1848 (1971); R.E. Olson, Phys. Rev. A6, 1822 (1972).
5. H.S.W. Massey, Rep. Prog. Phys. 12, 248 (1948).
6. J.B. Hasted, Proc. Roy, Soc. (London) A*205*, 421 (1951); H.G.Gilbody and J.B. Hasted, Proc. Roy. Soc. (London) A*238*, 334 (1956).
7. J. Perel and H.L. Daley, Phys. Rev. A4, 162 (1971).
8. D. Rapp and W.E. Francis, J. Chem. Phys. 37, 2631 (1962).
9. A.R. Lee and J.B. Hasted, Proc. Phys. Soc. (London) 85, 673 (1965).
10. T.R. Dinterman and J.B. Delos, Phys. Rev. A*15*, 463 (1977).
11. C.F. Melius and W.A. Goddard. Chem. Phys. Lett. *15*, 524 (1972);Phys. Rev. Lett. 29, 975 (1972); Phys. Rev. A*10*, 1541 (1974).
12. N. Matić, in *The Physics of Ionized Gases,* 195, ed. by R. K. Janev, Belgrade, Institute of Physics (1978).
13. R.J. Allan and J. Hanssen, J. Phys. B*18*, 1981 (1985).
14. F.W. Byron, M.N. McDermott and R. Novick, Phys. Rev. *134*A, 615(1964).
15. R.H. Garstang, J. Opt. Soc. Am. 52, 845 (1962)
16. S. Dworetsky, R. Novick, W.W.Smith and N. Tolk, Phys. Rev. Lett.*18*, 939 (1967).
17. H. Rosenthal and H.M. Foley, Phys. Rev. Lett. 23, 1480 (1969).
18. V.A. Ankudinov, S.V. Bobashev and V.I. Perel, Sov. Phys. JETP 33, 490 (1971).
19. O.B. Shpenik, A.N. Zavilopulo and I.P. Zapesochnyi, Sov. Phys. JETP *35*, 466 (1972).
20. V. Aquilanti, P. Casavecchia and G. Grossi in *Coherence and Correlation in Atomic Collisions* ed. by H. Kleinpoppen and J.F. Williams, Plenum, p.413 (1980).
21. V. Aquilanti, P. Casavecchia and G. Grossi, J. Chem. Phys. 68, 1499 (1978).
22. L.F.S. Coelho, PhD Thesis, Sussex University (1981).
23. J. Los, Chem. Phys. *29*, 151 (1978).

24. A. N. Nesmeyanov, *Vapour Pressure of the Chemical Elements*, Elsevier (1963).
25. R.E. Honig and D.A. Kramer, RCA Review 30, 1, 285 (1965).
26. N. Andersen and S.E. Nielsen, Adv. Atom. Mol. Phys. 18, 266 (1982).
27. P. Bisgaard, T. Andersen, B.V. Sorensen, S. E. Nielsen and J.S. Dahler, J. Phys. B*13*, 4441 (1980).
28. S.E. Nielsen, M. Larsen and J.S. Dahler, J. Phys. B*18*, 4095 (1985).
29. M. Kimura and R.E. Olson, J. Phys. B*18*, L617 (1985).
30. R. Shingal, B.H. Bransden, A.M. Ermolaev, D.R. Flower, C. W. Newby and C.J. Noble, J. Phys. B*19*, 309 (1986); R.J. Allan, J. Phys. B*19*, 321 (1986); R.J. Allan, R. Shingal and D.R. Flower, J. Phys. B 19, L251 (1986).
31. A.T. Martin, R.W. McCullough and H.B. Gilbody, unpublished results (1975), personal communication by Gilbody (1981).

Resumo

A seção de choque de emissão de 326.1 nm para o processo de colisão - $Cd^+ + Na \rightarrow Cd(5^3P_1) + Na$ - foi medida na faixa de energia de 1,5 a 4,9 keV. Ela decresce monotonamente de 5 até 2×10^{-15} cm^2. Devido à quase degenerescência em energia este canal apresenta uma seção de choque muito acima de todas as outras (com excessão dos canais de troca de carga para 5^3P_0 e 5^3P_2, os quais são altamente metaestáveis). Isto permite negligenciar o mecanismo de cascata para o aumento da população de átomos em 5^3P_1 e, consequentemente, resulta em identificar a seção de choque de emissão de 326.1 nm com a de excitação do estado 5^3P_1. Os valores medidos concordam bem com estimativas teóricas baseadas no modelo de Olson para troca de carga quase-ressonante.